ELSEVIER

Journal of Organometallic Chemistry 635 (2001) 197–203

Journal of Organometallic Chemistry

www.elsevier.com/locate/jorganchem

Bis(indenyl) complexes of Fe, Co, and Ni: electronic structure and preferences

Maria José Calhorda [a,b,*], Luís F. Veiros [c]

[a] *Instituto de Tecnologia Química e Biologica (ITQB), UNL, Av. da República, EAN, Apart. 127, 2781-901 Oeiras, Portugal*
[b] *Dep. Química e Bioquímica, Faculdade de Ciências, Universidade de Lisboa, 1749-016 Lisbon, Portugal*
[c] *Centro de Química Estrutural, Complexo I, Instituto Superior Técnico, Av. Rovisco Pais, 1, 1049-001 Lisbon, Portugal*

Received 23 April 2001; accepted 3 June 2001

Abstract

The bis(indenyl) derivatives of Fe, Co, and Ni were studied by means of DFT calculations (ADF program). The calculated structures were compared with the experimental ones and a good agreement was observed. While bis(indenyl)iron is an 18-electron compound, exhibiting an almost perfect η^5 coordination of the indenyl ring, the cobalt complex is a paramagnetic species, owing to the presence of an extra electron and structural distortions start to be detected. More interesting is the nickel complex, where the ring exhibits a coordination between $\eta^2+\eta^3$ and η^3, and is definitely slipped and folded. On the other hand, nickelocene chooses a distorted η^5 coordination with long Ni–C bonds and two unpaired electrons. This different behavior is related to the tendency of the indenyl to slip, compared to cyclopentadienyl. The geometry of the indenyl ring in bis(indenyl)nickel is useful to compare with that of non-isolable intermediates and transition states.

Keywords: Indenyl effect; Metallocenes; Iron; Cobalt; Nickel; DFT calculations

1. Introduction

The indenyl ligand has received much attention, mainly owing to the 'indenyl effect', a term introduced by Basolo et al., who noticed that when a cyclopentadienyl ring ($Cp = C_5H_5^-$) was replaced by an indenyl ring ($Ind = C_9H_7^-$) reaction rates were strongly accelerated [1]. Much work, both experimental [2] and theoretical [3], has been devoted to studying and comparing the behavior of the two (and other related) rings. The addition of two electrons, either by reduction or ligand addition, to a η^5-coordinated ring easily induces ring slippage in indenyl and large rings, which become η^3-coordinated, while Cp usually exhibits a different behavior [4]. The change in hapticity is accompanied by structural modifications, as has been described in detail before for several systems [5]. The binary bis(indenyl) complexes, on the other hand, have received less attention. Ind_2Fe is the analogue of ferrocene, and in both compounds η^5 rings are observed [6]. The cobalt derivative, having formally 19 electrons, is paramagnetic and exhibits the same arrangement as the iron analogues [6]. Nickel gives rise to the more interesting species in this small family. In order to accommodate the 20 electrons, nickelocene becomes paramagnetic (two unpaired electrons), the five Ni–C bonds being of similar length. On the other hand, in comparison with Ind_2Fe, the bis(indenyl) derivative experiences a distortion, which leads to some folding and slippage of the rings, which are staggered in the X-ray structure, and is diamagnetic [6].

In this work, we performed DFT calculations [7] (ADF program [8]) in order to explain the structural preferences of the Fe, Co, and Ni derivatives, and the factors determining the competition between ring slip-page and formation of a paramagnetic species. Bonding in these complexes is explained by the Dewar model initially introduced for olefin complexes [9], and consists of electron donation from the rings to the metal accompanied by back donation from metal to rings. The energies of the optimized structures were also calculated using the MP2 [10] approach (GAUSSIAN-98 [11]).

* Corresponding author. Tel.: +351-21-4469754; fax: +351-21-4411277.
E-mail address: mjc@itqb.unl.pt (M.J. Calhorda).

0022-328X/01/$ - see front matter
PII: S0022-328X(01)01064-6

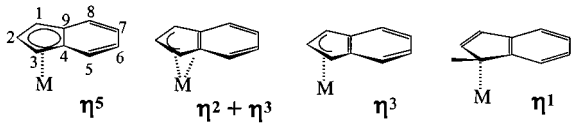

Scheme 1.

2. Results and discussion

2.1. Bis(indenyl)iron

Ind_2Fe exhibits a typical coordination of the indenyl ring, closer to a $\eta^2+\eta^3$ mode, than to a perfect η^5 mode (Scheme 1, also showing the atom numbering scheme of indenyl), as observed in the experimentally determined structure [6].

Two structural parameters are commonly used to describe the indenyl coordination, namely the M–C distances and the folding angle Ω, defined as the angle between the planes of carbons 1, 2, 3 and 1, 3, 4, 9 (also called the hinge angle) [6]. A perfect η^5 coordination is never observed for indenyl, although Ind_2Fe is certainly the closest approach, with the two distances Fe–C4,9 only slightly longer than the other three and a folding angle of $\sim 2.6°$ (Fig. 1). The two indenyl rings in the structure are eclipsed, so that the rotation angle is 0°. This is the angle between the two planes defined by the metal M, C2, and the C4–C9 midpoint, in each ligand. The eclipsed arrangement was calculated to be the most stable (by 5 kJ mol^{-1} from DFT calculations, and by 14 kJ mol^{-1} from MP2 calculations, without any symmetry constraints; see Section 4).

The calculated and the observed [6] structures are depicted in Fig. 1, along with some relevant distances and angles.

The calculated Fe–C distances, relative to the five-membered rings (2.036, 2.050, 2.050, 2.119, 2.118 Å in one ring, and 2.039, 2.053, 2.052, 2.122, and 2.122 Å in the other), agree extremely well with the experimental values (2.035, 2.042, 2.054, 2.092, 2.104 Å, and 2.041, 2.048, 2.049, 2.094, 2.100 Å, for each ring, respectively) [6]. There are some differences, namely, the rings are perfectly eclipsed in the calculated structure (notice that no symmetry constraints were introduced) and rotated 13.0° (or 5.2° in the second independent molecule of the unit cell) away from eclipsed in the crystal structure. These differences are probably caused by packing effects. The rings are practically planar, the folding angles being 2.9° (calculated) and 2.6°, 2.7° (experimental).

Ind_2Fe is a typical 18-electron species, analogous to ferrocene, and therefore no distortions are expected. The fact that the five Fe–C distances are not exactly similar can be explained on the basis of the different contributions of the five carbon atoms in the coordinating ring to the π-orbitals of indenyl which are relevant to the bonding. The extended Hückel [12] molecular orbital diagram (Scheme 2) shows the main interactions between iron and the two indenyl rings, which are essentially donations from the ring to the metal, back-donation being negligible.

The structure of the permethylated derivative $[(C_9Me_7)_2Fe]$ has also been determined and the rotation angle increased to 151.3°, relatively close to a staggered arrangement of the indenyl rings, but keeping the C5 coordinating rings eclipsed. This result is not too surprising, considering the very small energy difference calculated for the two forms, and indicates that steric repulsions between methyl groups are not determining the structure. The rings are still essentially planar, with a folding angle of 4.4°. A photoelectron spectroscopy study [13] combined with extended Hückel calculations showed the highest occupied molecular orbitals of these systems to be mainly localized on the metal, as depicted

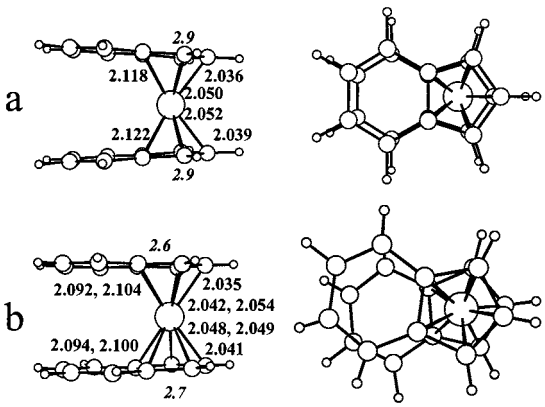

Fig. 1. Fe–C distances (Å) and folding angles (°) in the structure of Ind_2Fe in a side view and a top view: (a) DFT calculations and (b) X-ray structure.

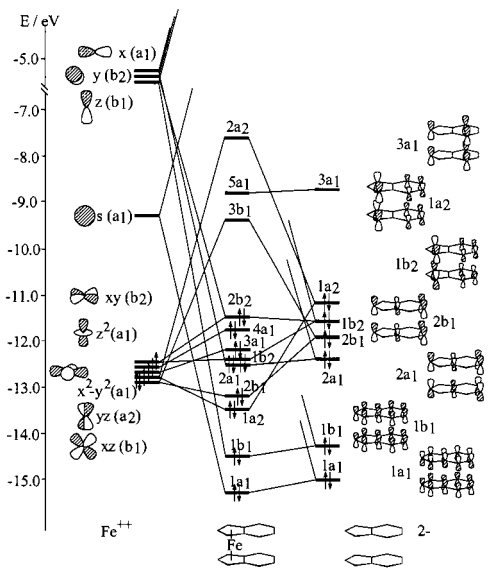

Scheme 2.

in our molecular orbital in Scheme 2. The related ansa-derivative [*trans*-$Ph_2C_2H_2$–*rac*-(η^5-4,7-Me–C_9H_4)$_2$-Fe], where the relative arrangement of the two indenyl rings is constrained by the C_2 bridge, exhibits an almost eclipsed arrangement [14].

2.2. Bis(indenyl)cobalt

The bis(indenyl)cobalt complex holds one more electron than Ind_2Fe, and is therefore paramagnetic [6,13]. The geometry was fully optimized without symmetry using DFT calculations (ADF), and the energy difference between the eclipsed and the staggered arrangement was only 5 kJ mol^{-1}, the staggered form being the most stable. However, MP2 calculations showed the eclipsed species to be more stable by 13 kJ mol^{-1}, in agreement with the results from the X-ray structure determination (Fig. 2).

The main features as well as the comparison between optimized and experimental structures resemble what was discussed for the iron derivative. In the X-ray structure, the two rings are moved 10.5° away from eclipsed (only 0.2° in the calculated form), and the coordination mode of the indenyl can still be classified as $\eta^2 + \eta^3$. There are significant changes, however. The range of calculated Co–C distances goes from 2.070 (C2), 2.072 (C1, C3), and 2.235 Å (C4, C9), while the observed ones range from 2.058 (C2), 2.079, 2.089 (C1, C3), and 2.182, 2.187 (C4, C9) in one ring to 2.059 (C2), 2.072, 2.085 (C1, C3), and 2.194, 2.197 Å (C4, C9) in the other. On the other hand, the calculated folding angle was 7.6° and the observed ones 7.4 and 7.8°. The calculated structure is more symmetric, despite the absence of symmetry constraints in the calculations, but the agreement is very good. Comparing these results with those relative to Ind_2Fe, three aspects can be noticed: the M–C distances are longer; the range of M–C distances is wider; and the folding angle is larger.

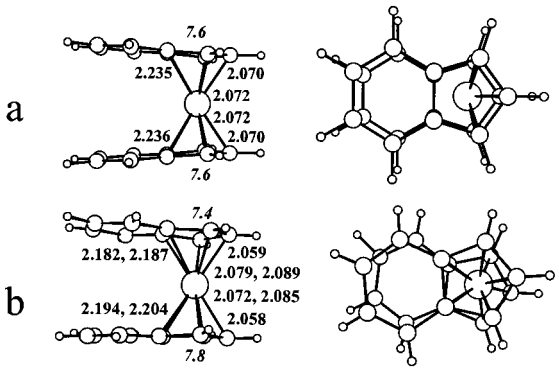

Fig. 2. Co–C distances (Å) and folding angles (°) in the structure of Ind_2Co in a side view and a top view: (a) DFT calculations and (b) X-ray structure.

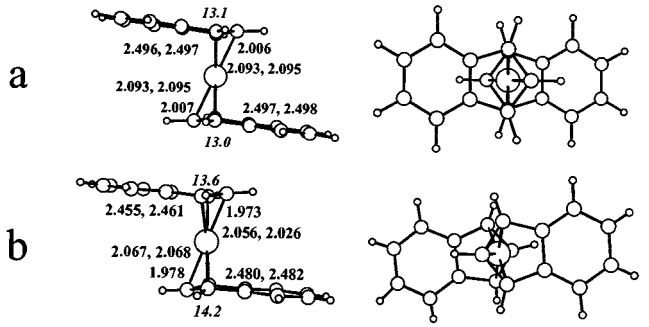

Fig. 3. Ni–C distances (Å) and folding angles (°) in the structure of Ind_2Ni in a side view and a top view: (a) DFT calculations and (b) X-ray structure.

The extra electron of Ind_2Co occupies an antibonding orbital (see Scheme 2), leading to longer M–C distances. The average Fe–C distances are 2.075, 2.078 (calculated) and 2.065, 2.066 Å (experimental), while Co–C distances are 2.137 (calculated) and 2.119, 2.123 Å (observed). The other two changes result from the tendency of indenyl to slip, in order to decrease the antibonding character of the new singly occupied HOMO, as will be discussed in more detail in the next section. For the time being, it is enough to notice that the folding starts to be significant, while two of the Co–C bonds are distinctly longer, and the $\eta^2 + \eta^3$ coordination mode is moving towards a pure η^3. Permethylated species have been prepared, but only the cationic [$(C_9Me_7)_2Co$][PF_6] was structurally characterized. As expected (one less antibonding electron) the Co–C distances are shorter (analogous to Fe–C in Ind_2Fe, namely an average 2.077 Å), but the rotation angle is 89° [15]. These angles appear to be randomly distributed, reflecting the small energy differences calculated for the two extreme conformations.

2.3. Bis(indenyl)nickel

The X-ray structure of Ind_2Ni exhibits a staggered arrangement, in opposition to the Fe and Co derivatives. The indenyl rings are also more distorted. Geometry optimizations (DFT, ADF) performed in the same conditions, led to a lower energy for the staggered arrangement relative to the eclipsed one (8 kJ mol^{-1}, DFT; 3 kJ mol^{-1}, MP2/6-31G*; 24 kJ mol^{-1}, MP2/6-31G**), which is shown in Fig. 3.

The distortion of the indenyl (folding), which becomes apparent in Ind_2Co, is now clear, with folding angles Ω of 13° (calculated) and 14° (X-ray structure). The coordination mode is closer to η^3 than $\eta^2 + \eta^3$, since two Ni–C distances in each ring approach 2.5 Å, which is a long distance for a Ni–C bond, indicating weak bonds. The origin of this slippage and folding of the indenyl can be qualitatively traced to the occupation by two electrons of a Ni–indenyl antibonding

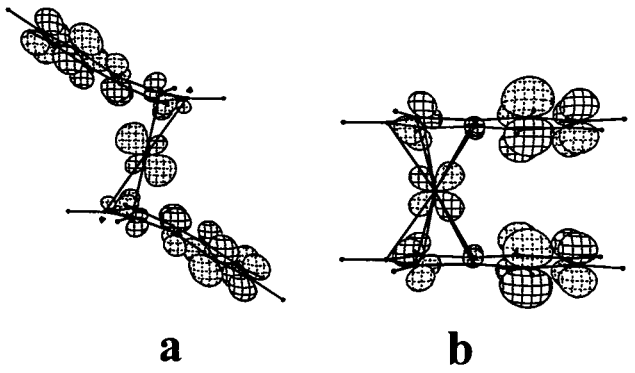

Fig. 4. Three-dimensional representations of: (a) the HOMO of Ind_2Ni and (b) the LUMO of Ind_2Fe.

Table 1
Relative energies (kJ mol^{-1}) for Ind_2Ni and Cp_2Ni complexes, diamagnetic and paramagnetic, with eclipsed or staggered arrangements of the rings

	Diamagnetic		Paramagnetic	
	Eclipsed	Staggered	Eclipsed	Staggered
Ind_2Ni [a]	3.0	0.0	5.5	0.3
Cp_2Ni [b]	160.9	[c]	4.5	0.0
	139.7 [d]	132.2 [d]		

[a] MP2/6-31G*.
[b] MP2/6-31G**.
[c] Convergence was not achieved.
[d] In this calculation, the cyclopentadienyl ring was folded (30°) in the starting geometry; in all the others, it was planar.

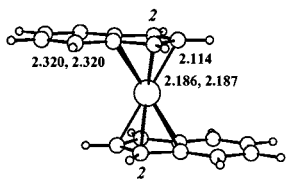

Fig. 5. Ni–C distances (Å) in the structure of a paramagnetic Ind_2Ni complex in a side view (DFT calculations).

orbital. Slippage releases part of this antibonding character, as mentioned above for Ind_2Co. The HOMO of Ind_2Ni is shown in Fig. 4(a) and compared to the LUMO of Ind_2Fe (Fig. 4(b)). Both were calculated using the extended Hückel method [12,16].

The observation of the HOMO of Ind_2Ni also leads to the understanding of the preference for a staggered arrangement of the ring. The metal xz orbital mixes with z^2 in such a way as to minimize the Ni–C antibonding character. The folding of the indenyl also helps relieve that antibonding character by contributing to an increased distance between Ni and the carbon atoms of the junction (C4, C9).

This geometry can be compared with others, assuming that in Ind_2Ni each indenyl ring has received an average of one electron per ring. This same situation is observed in the calculated (DFT) structure of the paramagnetic one-electron reduction product of $[Mo(\eta^5\text{-}Cp)(\eta^5\text{-}Ind)\{P(OMe)_3\}_2]^{2+}$ ($\Omega = 11°$) where the Mo–C(4,9) distances are 2.788 Å, midway between those observed in the η^5-indenyl ring (2.469, 2.522 Å) and in the η^3-indenyl ring of the doubly reduced complex (3.063 Å) [3o]. Another example is found in the calculated transition state (DFT/B3LYP) for the indenyl slippage induced by phosphine addition to $[Mn(\eta^5\text{-}Ind)(CO)_3]$. At the transition state, the reaction is approximately in the middle, and again the Mn–C(4,9) distances (2.752 and 2.849 Å) and the folding angle ($\Omega = 17°$) are intermediate between those of the parent complex ($\Omega = 5°$, 2.237 Å) and those of the final product ($\Omega = 24°$, 3.008 Å) [3n].

The alternative structure which allowed the complex to become paramagnetic, with two electrons occupying the two LUMOs $3b_1$ and $5a_1$ (Scheme 2), was also investigated. The relative energies of the several arrangements studied are given in Table 1, both for Ind_2Ni and for Cp_2Ni, to be addressed below. Although all the optimizations were performed using DFT calculations, it was found that for these groups of compounds the DFT energies were not reliable. Therefore, only MP2 energies are given in Table 1.

For the bis(indenyl) derivatives, the energies do not differ very significantly, staggered arrangements being always preferred, both for diamagnetic and for paramagnetic species. The geometry of the most stable paramagnetic structure is given in Fig. 5.

The Ni–C distances are all relatively long, which is not surprising considering the antibonding character of the two singly occupied HOMOs, the two distances to C4 and C9 being significantly longer than the other three (which are much longer than in Ind_2Co). On the other hand, the indenyl is almost perfectly planar, and the coordination mode a typical $\eta^2 + \eta^3$. The preferences are not very well defined. We can assign, however, the choice of the slipped, diamagnetic arrangement to the easy way in which the indenyl ring slips and folds. This leads us to the analysis of bis(cyclopentadienyl)nickel, a well known paramagnetic 20-electron compound. The values in Table 1 show that this is indeed the preferred structure of nickelocene [17], the paramagnetic species being preferred by ca. 150 kJ mol^{-1}, and the staggered by 5 kJ mol^{-1} relative to the eclipsed. The high energy of the diamagnetic form led to convergence problems when trying to optimize the geometry and explains why another, more favorable, geometry was also used as a starting geometry. The geometries and most relevant distances are given in Fig. 6 for the most stable paramagnetic form, the X-ray structure, and the lowest energy diamagnetic isomer.

The energetic balance between paramagnetic and diamagnetic species is very different for the indenyl and

the cyclopentadienyl rings, the energy differences being much wider for the Cp. This different behavior is related to the so-called 'indenyl effect' [1] and can be traced to the different binding energies of the η^5 and η^3 rings to a metal [3l]. Cp is a stronger η^5 coordinating ligand than indenyl, but a weaker η^3 coordinating ligand. Indenyl will easily undergo a slippage and folding distortion as antibonding electrons are added, when going from the iron metallocenes, to the cobalt, and to the nickel ones. Cp, very strongly bound as an η^5 ligand, will try to avoid losing this coordination.

A spin equilibrium between a diamagnetic and a paramagnetic species has been described for (C_5Me_5)-Ni(acac) [18]. The electronic situation is different, however, as this is formally an 18-electron complex. The coordination of a π-donor to the metal, in comparison to the more ubiquitous, π-acceptor, carbonyl, leads to a very small HOMO–LUMO gap [19]. The diamagnetic form with a doubly occupied HOMO is competitive to the paramagnetic form where both HOMO and LUMO carry one electron.

3. Conclusions

The structures of Ind_2M (M = Fe, Co, Ni) exhibit a progressively more distorted coordination of the indenyl ring, as one goes from Fe, to Co, and to Ni. The extra electrons occupy one antibonding orbital which becomes less antibonding when the indenyl slips and folds, moving towards an η^3 coordination, but not achieving it in this triad, as there are not enough electrons (two electrons per ring). On the other hand, nickelocene exhibits an almost undistorted coordination of the Cp ring (planar and almost η^5), with two electrons with the same spin in antibonding orbitals, in accordance with its paramagnetic behavior. This alternative behavior reflects the different binding capacities of the two rings in η^5 and η^3 modes. Eclipsed and staggered arrangements of the rings differ by very small amounts for the Fe and Co indenyl complexes, the staggered arrangement being decidedly preferred for nickel metallocenes.

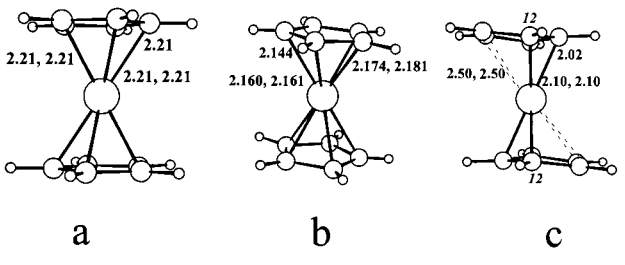

Fig. 6. Ni–C distances (Å) and folding angles (°) in the structure of Cp_2Ni: (a) DFT calculations, paramagnetic; (b) X-ray structure; and (c) DFT calculations, diamagnetic.

4. Computational details

4.1. DFT calculations

Density functional calculations [7] were carried out with the Amsterdam Density Functional (ADF2000) program developed by Baerends and coworkers [8]. The local exchange correlation potential developed by Vosko et al. [20] was used. Gradient corrected geometry optimizations [21] were performed using the Generalized Gradient Approximation (Becke's exchange [22] and Perdew's [23] correlation functionals). Unrestricted calculations were performed for all the paramagnetic species studied.

The inner shells of Fe ([1–2]s, 2p), Co ([1–2]s, 2p), Fe ([1–2]s, 2p), and C (1s) were frozen. An uncontracted triple-ζ nd, $(n+1)$s STO basis set was used for Fe, Co, and Ni, augmented by one $(n+1)$p function. The valence shells for C (2s, 2p) was described by an uncontracted triple-ζ STO basis set, augmented by two polarization functions: 3d and 4f. For H an uncontracted triple-ζ STO basis set (1s) with two polarization functions, 2p and 3d, was used. Full geometry optimizations were performed without any symmetry constraints on models based on the available crystal structures, as described in the text.

4.2. MP2 calculations

Single point calculations were performed by means of ab initio calculations with the GAUSSIAN-98 program [11] at the second-order Møller–Plesset (MP2) level [10] with a 6-31G** basis set [24] in the case of nickelocenes, and 6-31G* [24] for all the indenyl derivatives of Fe, Co, and Ni. Spin contamination was carefully monitored in all the unrestricted calculations performed for the paramagnetic species, and the values of $\langle S^2 \rangle$ indicate minor spin contamination: between 0.75 and 0.79 for the Co complexes and 2.000 for the Ni complexes.

4.3. Extended Hückel calculations

The extended Hückel calculations [12] were performed using the CACAO program [16] with modified H_{ij} values [25]. The basis set for the metal atoms consisted of ns, np and $(n-1)$d orbitals. The s and p orbitals were described by single Slater-type wave functions, and the d orbitals were taken as contracted linear combinations of two Slater-type wave functions. The parameters used for the transition metals were the following (H_{ii} (eV), ζ): 4s −9.17, 1.900; 4p −5.37, 1.900; 3d −12.70, 5.350, 1.800 (ζ_2), 0.5366 (C_1), 0.6678 (C_2), for Fe; 4s −9.54, 2.000; 4p −4.51, 2.000; 3d −12.48, 5.550, 2.100 (ζ_2), 0.5680 (C_1), 0.6060 (C_2), for Co, and 4s −9.11, 1.825; 4p −5.15, 1.125; 3d −13.40,

5.750, 2.000 (ζ_2), 0.5683 (C_1), 0.6292 (C_2), for Ni. Standard parameters were used for other atoms. Calculations were performed on models based on the crystal structures with idealized maximum symmetry, and the following distances (Å): M–C_5(ring centroid) 1.67, C–C 1.40, C–H 1.08; the η^3 coordination of indenyl was modeled by a $\Omega = 30°$ folding angle.

References

[1] M.E. Rerek, L.-N. Ji, F. Basolo, J. Chem. Soc. Chem. Commun. (1983) 1208.

[2] (a) L.-N. Ji, M.E. Rerek, F. Basolo, Organometallics 3 (1984) 740;
(b) W. Simanko, V.N. Sapunov, R. Schmid, K. Kirchner, S. Wherland, Organometallics 17 (1998) 2391;
(c) E.U. Van Raaij, H.H. Brintzinger, L. Zsolnai, G. Huttner, Z. anorg. allg. Chem. 577 (1989) 217;
(d) R.M. Kowalewski, A.L. Rheingold, W.C. Trogler, F. Basolo, J. Am. Chem. Soc. 108 (1986) 2460;
(e) Z. Zhou, C. Jablonski, J. Brisdon, J. Organomet. Chem. 461 (1993) 215;
(f) D.A. Brown, N.J. Fitzpatrick, W.K. Glass, H.A. Ahmed, D. Cunningham, P. McArdle, J. Organomet. Chem. 455 (1993) 157;
(g) K.A. Pevear, M.M. Banaszak Holl, G.B. Carpenter, A.L. Rieger, P.H. Rieger, D.A. Sweigart, Organometallics 14 (1995) 512;
(h) J.S. Merola, R.T. Kacmarcik, D. Van Engen, J. Am. Chem. Soc. 108 (1986) 329;
(i) R. Poli, S.P. Mattamana, L.R. Falvello, Gazz. Chim. Ital. 122 (1992) 315;
(j) J.R. Ascenso, C.G. Azevedo, I.S. Gonçalves, E. Herdtweck, D.S. Moreno, C.C. Romão, J. Zühlke, Organometallics 13 (1994) 429;
(k) I.S. Gonçalves, C.C. Romão, J. Organomet. Chem. 486 (1995) 155;
(l) J.W. Faller, R.H. Crabtree, A. Habib, Organometallics 4 (1985) 929;
(m) T.A. Huber, M. Bayrakdarian, S. Dion, I. Dubuc, F. Bélanger-Gariépy, D. Zargarian, Organometallics 16 (1997) 5811;
(n) R.H. Crabtree, C.P. Panell, Organometallics 3 (1984) 1727;
(o) T.B. Marder, J.C. Calabrese, D.C. Roe, T.H. Tulip, Organometallics 6 (1987) 2012;
(p) A. Georg, C.G. Kreiter, Eur. J. Inorg. Chem. (1999) 651;
(q) G.J. Kubas, G. Kiss, C.D. Hoff, Organometallics 10 (1991) 2870;
(r) R.N. Biagioni, I.M. Lorkovic, J. Skelton, J.B. Hartung, Organometallics 9 (1990) 547;
(s) A. Decken, S.S. Rigby, L. Girard, A.D. Bain, M.J. McGlinchey, Organometallics 16 (1997) 1308;
(t) G.M. Diamond, M.L.H. Green, P. Mountford, N.A. Popham, A.N. Chernega, J. Chem. Soc. Chem. Commun. (1994) 103;
(u) M. Bochmann, S.J. Lancaster, M.B. Hursthouse, M. Mazid, Organometallics 12 (1993) 4718;
(v) R.T. Baker, T.H. Tulip, Organometallics 5 (1986) 839;
(x) F.H. Köhler, Chem. Ber. 107 (1974) 570.

[3] (a) A. Decken, J.F. Britten, M.J. McGlinchey, J. Am. Chem. Soc. 115 (1993) 7275;
(b) A. Decken, S.S. Rigby, L. Girard, A.D. Bain, M.J. McGlinchey, Organometallics 16 (1997) 1308;
(c) T.A. Albright, P. Hofmann, R. Hoffmann, C.P. Lillya, P.A. Dobosh, J. Am. Chem. Soc. 105 (1983) 3396;
(d) A.K. Kakkar, N.J. Taylor, J.C. Calabrese, W.A. Nugent, D.C. Roe, E.A. Connaway, T.B. Marder, J. Chem. Soc. Chem. Commun. (1989) 990;
(e) N.S. Crossley, J.C. Green, A. Nagy, G. Stringer, J. Chem. Soc. Dalton Trans. (1989) 2139;
(f) T.M. Frankcom, J.C. Green, A. Nagy, A.K. Kakkar, T.B. Marder, Organometallics 12 (1993) 3688;
(g) J.C. Green, R.P.G. Parkin, X. Yang, A. Haaland, W. Scherer, M. Tapifolsky, J. Chem. Soc. Dalton Trans. (1997) 3219;
(h) C.N. Field, J.C. Green, A.G.J. Moody, M.R.F. Siggel, Chem. Phys. 206 (1996) 211;
(i) C. Bonifaci, A. Ceccon, S. Santi, C. Mealli, R.W. Zoellner, Inorg. Chim. Acta 240 (1995) 541;
(j) M.J. Calhorda, L.F. Veiros, Coord. Chem. Rev. 185–186 (1999) 37;
(k) M.J. Calhorda, C.A. Gamelas, I.S. Gonçalves, E. Herdtweck, C.C. Romão, L.F. Veiros, Organometallics 17 (1998) 2597;
(l) M.J. Calhorda, C.A. Gamelas, C.C. Romão, L.F. Veiros, Eur. J. Inorg. Chem. (2000) 331;
(m) L.F. Veiros, J. Organomet. Chem. 587 (1999) 221;
(n) L.F. Veiros, Organometallics 19 (2000) 3127;
(o) M.E. Stoll, P. Belanzoni, M.J. Calhorda, M.G.B. Drew, V. Félix, W.E. Geiger, C.A. Gamelas, I.S. Gonçalves, C.C. Romão, L.F. Veiros, J. Am. Chem. Soc. (accepted).

[4] L.F. Veiros, Organometallics 19 (2000) 5549.

[5] M.J. Calhorda, L.F. Veiros, Comments Inorg. Chem., in press.

[6] S.A. Westcott, A.K. Kakkar, G. Stringer, N.J. Taylor, T.B. Marder, J. Organomet. Chem. 394 (1990) 777.

[7] R.G. Parr, W. Yang, Density Functional Theory of Atoms and Molecules, Oxford University Press, New York, 1989.

[8] (a) E.J. Baerends, A. Bérces, C. Bo, P.M. Boerrigter, L. Cavallo, L. Deng, R.M. Dickson, D.E. Ellis, L. Fan, T.H. Fischer, C. Fonseca Guerra, S.J.A. van Gisbergen, J.A. Groeneveld, O.V. Gritsenko, F.E. Harris, P. van den Hoek, H. Jacobsen, G. van Kessel, F. Kootstra, E. van Lenthe, V.P. Osinga, P.H.T. Philipsen, D. Post, C.C. Pye, W. Ravenek, P. Ros, P.R.T. Schipper, G. Schreckenbach, J.G. Snijders, M. Sola, D. Swerhone, G. te Velde, P. Vernooijs, L. Versluis, O. Visser, E. van Wezenbeek, G. Wiesenekker, S.K. Wolff, T.K. Woo, T. Ziegler, ADF2000;
(b) C. Fonseca Guerra, O. Visser, J.G. Snijders, G. te Velde, E.J. Baerends, Parallelisation of the Amsterdam Density Functional Programme, in: E. Clementi, C. Corongiu (Eds.), Methods and Techniques for Computational Chemistry, STEF, Cagliari, 1995, pp. 303–395;
(c) C. Fonseca Guerra, J.G. Snijders, G. te Velde, E.J. Baerends, Theor. Chem. Acc. 99 (1998) 391;
(d) E.J. Baerends, D. Ellis, P. Ros, Chem. Phys. 2 (1973) 41;
(e) E.J. Baerends, P. Ros, Int. J. Quantum Chem. S12 (1978) 169;
(f) P.M. Boerrigter, G. te Velde, E.J. Baerends, Int. J. Quantum Chem. 33 (1988) 87;
(g) G. te Velde, E.J. Baerends, J. Comp. Phys. 99 (1992) 84.

[9] J.S. Dewar, Bull. Soc. Chim. Fr. 18 (1951) C71.

[10] (a) C. Møller, M.S. Plesset, Phys. Rev. 46 (1934) 618;
(b) J.S. Binkley, J.A. Pople, Int. J. Quantum Chem. 9 (1975) 229;
(c) J.S. Binkley, J.A. Pople, R. Seeger, Int. J. Quantum Chem. S10 (1976) 1;
(d) R. Krishnan, J.A. Pople, Int. J. Quantum Chem. 14 (1978) 91;
(e) R. Krishnan, M. Frisch, J.A. Pople, J. Chem. Phys. 72 (1980) 4244.

[11] M.J. Frisch, G.W. Trucks, H.B. Schlegel, G.E. Scuseria, M.A. Robb, J.R. Cheeseman, V.G. Zakrzewski, J.A. Montgomery Jr., R.E. Stratmann, J.C. Burant, S. Dapprich, J.M. Millam, A.D. Daniels, K.N. Kudin, M.C. Strain, O. Farkas, J. Tomasi, V.

Barone, M. Cossi, R. Cammi, B. Mennucci, C. Pomelli, C. Adamo, S. Clifford, J. Ochterski, G.A. Petersson, P.Y. Ayala, Q. Cui, K. Morokuma, D.K. Malick, A.D. Rabuck, K. Raghavachari, J.B. Foresman, J. Cioslowski, J.V. Ortiz, B.B. Stefanov, G. Liu, A. Liashenko, P. Piskorz, I. Komaromi, R. Gomperts, R.L. Martin, D.J. Fox, T. Keith, M.A. Al-Laham, C.Y. Peng, A. Nanayakkara, C. Gonzalez, M. Challacombe, P.M.W. Gill, B. Johnson, W. Chen, M.W. Wong, J.L. Andres, C. Gonzalez, M. Head-Gordon, E.S. Replogle, J.A. Pople, GAUSSIAN-98, Revision A.6, Gaussian, Inc., Pittsburgh PA, 1998.

[12] (a) R. Hoffmann, J. Chem. Phys. 39 (1963) 1397;
(b) R. Hoffmann, W.N. Lipscomb, J. Chem. Phys. 36 (1962) 2179.

[13] D. O'Hare, J.C. Green, T. Marder, S. Collins, G. Stringer, A.K. Kakkar, N. Kaltsoyannis, A. Kuhn, R. Lewis, C. Mehnert, P. Scott, M. Kurmoo, S. Pugh, Organometallics 11 (1992) 48.

[14] P.J. Shapiro, K.M. Kane, A. Vij, D. Stelck, G.J. Matare, R.L. Hubbard, B. Caron, Organometallics 18 (1999) 3468.

[15] D. O'Hare, V.J. Murphy, N. Kaltsoyannis, J. Chem. Soc. Dalton Trans. (1993) 383.

[16] C. Mealli, D.M. Proserpio, J. Chem. Educ. 67 (1990) 39.

[17] P. Seiler, J.D. Dunitz, Acta Crystallogr. Sect. B 36 (1980) 2255.

[18] (a) M.E. Smith, R.A. Andersen, J. Am. Chem. Soc. 118 (1996) 11119;
(b) P.L. Holland, M.E. Smith, R.A. Andersen, R.G. Bergman, J. Am. Chem. Soc. 118 (1996) 12815.

[19] T.A. Albright, J.K. Burdett, M.-H. Whangbo, Orbital Interactions in Chemistry, Wiley, New York, 1985.

[20] S.H. Vosko, L. Wilk, M. Nusair, Can. J. Phys. 58 (1980) 1200.

[21] (a) L. Versluis, T. Ziegler, J. Chem. Phys. 88 (1988) 322;
(b) L. Fan, T. Ziegler, J. Chem. Phys. 95 (1991) 7401.

[22] A.D. Becke, J. Chem. Phys. 88 (1987) 1053.

[23] (a) J.P. Perdew, Phys. Rev. B 33 (1986) 8822;
(b) J.P. Perdew, Phys. Rev. B 34 (1986) 7406.

[24] (a) R. Ditchfield, W.J. Hehre, J.A. Pople, J. Chem. Phys. 54 (1971) 724;
(b) W.J. Hehre, R. Ditchfield, J.A. Pople, J. Chem. Phys. 56 (1972) 2257;
(c) P.C. Hariharan, J.A. Pople, Mol. Phys. 27 (1974) 209;
(d) M.S. Gordon, Chem. Phys. Lett. 76 (1980) 163;
(e) P.C. Hariharan, J.A. Pople, Theor. Chim. Acta 28 (1973) 213.

[25] J.H. Ammeter, H.-J. Bürgi, J.C. Thibeault, R. Hoffmann, J. Am. Chem. Soc. 100 (1978) 3686.